TECHNICAL PAPER

ISSN:1047-3289 *J. Air & Waste Manage. Assoc.* **59**:553–559
DOI:10.3155/1047-3289.59.5.553

Measurement and Capture of Fine and Ultrafine Particles from a Pilot-Scale Pulverized Coal Combustor with an Electrostatic Precipitator

Ying Li, Achariya Suriyawong, and Michael Daukoru
Aerosol and Air Quality Research Laboratory, Department of Energy, Environmental and Chemical Engineering, Washington University, St. Louis, MO

Ye Zhuang
Energy and Environmental Research Center, University of North Dakota, Grand Forks, ND

Pratim Biswas
Aerosol and Air Quality Research Laboratory, Department of Energy, Environmental and Chemical Engineering, Washington University, St. Louis, MO

ABSTRACT
Experiments were carried out in a pilot-scale pulverized coal combustor at the Energy and Environmental Research Center (EERC) burning a Powder River Basin (PRB) subbituminous coal. A scanning mobility particle sizer (SMPS) and an electrical low-pressure impactor (ELPI) were used to measure the particle size distributions (PSDs) in the range of 17 nm to 10 μm at the inlet and outlet of the electrostatic precipitator (ESP). At the ESP inlet, a high number concentration of ultrafine particles was found, with the peak at approximately 75 nm. A trimodal PSD for mass concentration was observed with the modes at approximately 80–100 nm, 1–2 μm, and 10 μm. The penetration of ultrafine particles through the ESP increased dramatically as particle size decreased below 70 nm, attributable to insufficient or partial charging of the ultrafine particles. Injection of nanostructured fine-particle sorbents for capture of toxic metals in the flue gas caused high penetration of the ultrafine particles through the ESP. The conventional ESP was modified to enhance charging using soft X-ray irradiation. A slipstream of flue gas was introduced from the pilot-scale facility and passed through this modified ESP. Enhancement of particle capture was observed with the soft X-ray irradiation when moderate voltages were used in the ESP, indicating more efficient charging of fine particles.

IMPLICATIONS
Emissions of fine and ultrafine particles from pulverized coal combustors are potentially of great concern. The pilot-scale results reported in this paper contribute to a better understanding of the PSDs that result in the combustion of subbituminous coals. It is confirmed that penetration of ultrafine particles (particularly those <50 nm) through conventional ESPs can be significant. This paper also provides useful strategies of how to enhance the capture of ultrafine particles.

INTRODUCTION
Significant research is currently underway related to particulate matter (PM) exposure and its adverse effects on human health. Fine ($d < 2.5$ μm) and ultrafine ($d < 0.1$ μm) particles are of special interest because they can penetrate into the alveolar regions of the lungs upon inhalation. It has been demonstrated that fine particles are associated with increased symptoms and deaths from cardiovascular and respiratory causes.[1–4] In 1997, the U.S. Environmental Protection Agency established a regulation of $PM_{2.5}$ (particles <2.5 μm in aerodynamic diameter) in addition to the existing PM_{10} (particles <10 μm in aerodynamic diameter) standards.[5] One of the major anthropogenic sources of $PM_{2.5}$ in the atmosphere is direct emissions from stationary combustion systems (utility and industrial boilers, incinerators, cooking, residential combustors, and others).[1] One of the largest source categories is electric utility coal combustion, accounting for 570,000 t/yr of $PM_{2.5}$ emissions in the United States in 2001.[6] To help reduce the emissions of fine particles and to protect public health, it is important to characterize particle size distributions (PSDs) from coal-fired utility boilers, especially in the fine and ultrafine size fractions.

Laboratory, pilot-, and full-scale studies have been conducted previously to measure the PSDs from pulverized coal combustors, which showed emissions of a significant fraction of fine/ultrafine particles before PM control devices; for example, electrostatic precipitators (ESPs) and/or baghouses. Zhuang and Biswas[7] studied submicrometer particle formation in a bench-scale pulverized coal combustor and found that the geometric mean particle size (on the basis of number concentration) ranges from 63 to 84 nm, which is consistent with a vaporization-nucleation-condensation formation and growth mechanism. Chang et al.[8] measured ultrafine PSDs from a pilot-scale coal-fired combustor and observed that the peak of particle number concentrations for medium sulfur bituminous coal was at 40–50 nm. Linak and Miller[9] observed trimodal PSDs (peaks at 0.07–0.08, 0.8–2, and

7–10 μm on the basis of mass concentration) when burning one subbituminous and two bituminous coal seams in a 50-kW pulverized coal combustor. Yoo et al.[10] observed bimodal PSDs (peaks at 0.1–1 and 5–10 μm) when burning one anthracite and two bituminous coal seams in a commercial coal-fired boiler, in which the PSD of the anthracite facility showed a distinct mode near 0.1 μm. Although most of the above literature reported PSDs burning bituminous coals, few data are available on burning subbituminous coals. Subbituminous coals account for the second largest U.S. coal reserves, with Powder River Basin (PRB) coal being the major source. Quann et al.[11] reported chemical composition of combustion-generated submicron particles for 11 coals, including two subbituminous coals; however, no details on PSDs were reported. Senior et al.[12] studied pilot-scale combustion of a PRB coal and reported that particles in the submicrometer range centered at 80 nm. However, data for particles smaller than 40 nm were not reported. Hence, a more comprehensive study is needed on the resultant PSDs obtained on burning subbituminous coal seams, particularly PRB coal.

ESPs are widely used as particulate control devices in industry, and their overall mass collection efficiency typically exceeds 99%.[13] However, there is a theoretical minimum collection efficiency in the size range of 0.1–1 μm because of the combination effect of diffusion charging (increase with decreased particle size) and field charging (increase with increased particle size).[14,15] Correspondingly, a "penetration window" is observed in the submicrometer range, in which the ESP collection efficiency can reach as low as 70–80%.[16–18] Contrary to the theoretical calculations,[14] many experimental observations have shown that ESP collection efficiency decreases with decreasing particle diameter in the ultrafine size range. Zhuang et al.[19] tested a laboratory-scale cylindrical ESP using aluminum oxide (Al_2O_3) and sodium chloride (NaCl) particles and found a decrease in collection efficiency as the particle size decreases below 100 nm. Huang and Chen[13] studied the ESP performance using monodisperse sucrose particles (in the range of 10–60 nm) and reported that aerosol penetration through their single- and two-stage ESPs increased significantly for particles below 20 and 50 nm, respectively. Yoo et al.[18] reported that the collection efficiency of a two-stage ESP decreases significantly for NaCl particles below 30 nm. Suriyawong et al.[20] studied charging and electrostatic collection of coal-combustion particles in laboratory experiments and reported that natural particle charging within the combustor itself is very low and that penetration of combustion particles increases as particle size decreases below 40 nm, regardless of the combustion gases used (air or oxygen-carbon dioxide mixtures). It should be noted that most of the above findings were based on bench-scale studies. Very few studies[17,21] have been reported on the penetration characteristics of pilot- and full-scale ESPs in the ultrafine size range. Hence, more studies on larger scale ESPs are needed and are now feasible because of the availability of several real-time fine PSD measurement instruments. In addition, the technology of sorbent particle injection in full-scale power plants is being proposed for the capture of certain toxic metals in the combustor.[22] For example, in situ-generated titanium dioxide (TiO_2) agglomerates, created by injecting titanium isopropoxide (TTIP) as the precursor, exhibited high efficiency in capturing gas-phase mercury in combustion flue gas.[23–25] The sizes of primary TiO_2 particles and TiO_2 agglomerates are approximately 5 and 200 nm, respectively.[25] Before large-scale use of such sorbents, the effectiveness of the ESP system to trap these materials is to be established. The results will provide for feasible size ranges of sorbents that can be readily used in such systems.

Because the bench-scale studies concluded that the significant decrease in collection efficiency of ultrafine particles was caused by partial or insufficient charging,[7,13,18] methods of charging ultrafine particles more efficiently are needed. Soft X-ray irradiation has been recently applied to effectively improve nanoparticle charging in several laboratory-scale studies.[26–28] X-ray radiation can charge the particles by two mechanisms: direct photoelectric charging and diffusion charging.[26,28,29] In direct photoelectric charging, the atoms or molecules on the surface of the aerosol particle are photoionized, whereas in diffusion charging the gas molecules are ionized by the radiation and then attach to the particles, resulting in their electrical charging. To the best of our knowledge, no study has examined the effectiveness of soft X-ray in enhancing ultrafine particle capture in pilot-scale coal combustors.

This paper reports experimental results from studies conducted on a pilot-scale pulverized coal combustor. Four aspects were studied: (1) resultant PSDs on burning a PRB subbituminous coal, measured before and after the pilot-scale ESP; (2) ESP collection efficiency as a function of particle size, particularly penetration of fine and ultrafine particles across the ESP; (3) ESP performance in the scenario of sorbent injection; and (4) the effect of soft X-ray irradiation on ultrafine particle capture conducted on a slipstream taken from the combustor.

EXPERIMENTAL METHODS

Description of the Pilot-Scale Coal Combustor

The experiments were conducted burning PRB subbituminous coal in a pilot-scale unit at the Energy and Environmental Research Center (EERC) at the University of North Dakota. It is a 160-kW pulverized coal-fired unit designed to generate fly ash representative of that produced in a full-scale utility boiler. The combustor is oriented vertically to minimize wall deposits. A refractory lining helps to ensure adequate flame temperature for complete combustion and prevents rapid quenching of the coalescing or condensing fly ash. The coal nozzle fires axially upward from the bottom of the combustor. The flue gas flow rate was 130 standard cubic feet per minute (scfm), or 210 $N \cdot m^3/hr$, and the mean residence time of a coal particle in the combustor was approximately 3 sec. A single-wire, tubular ESP (denoted as EERC-ESP) with a wire-to-tube spacing of 28 cm is used to collect fly ash particles. The EERC-ESP was operated at 40–60 kV with a corona current of approximately 4 mA. The actual plate current was continuously monitored to ensure consistent operation of the EERC-ESP from test to test. Downstream of the EERC-ESP is a heat-traced and insulated baghouse. It contains three bags (length = 400 cm; diameter = 13 cm), and each

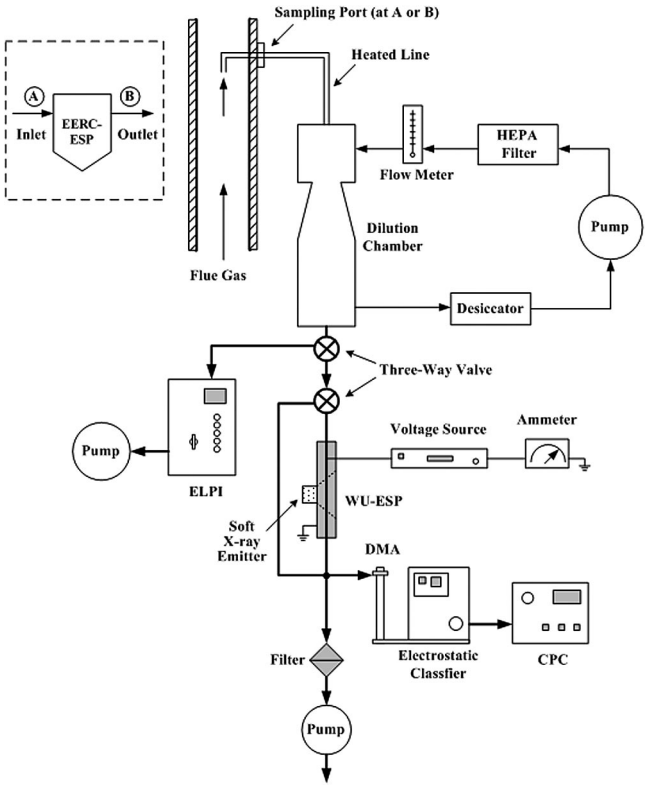

Figure 1. Schematic diagram of PM sampling system.

bag is cleaned separately with its own diaphragm pulse valve.

Apparatus and Methods

The schematic diagram of the PM sampling system is shown in Figure 1. PM samples were isokinetically collected from the flue gas at both EERC-ESP inlet and outlet, where the flue gas temperature was approximately 150 °C. The sampling line was heated to prevent thermophoretic deposition of particles. The sample was then diluted in a dilution chamber, where the dilution gas was circulated as shown in Figure 1. The dilution gas was drawn by a pump from the bottom of the dilution chamber and then treated in a desiccator to remove moisture. The gas then passed through a high-efficiency particulate air (HEPA) filter to remove all particles. The particulate-free gas was finally introduced to the top of the dilution chamber and the dilution cycle was complete. The flow rate of the dilution gas was measured by a flow meter and maintained around 40 L/min. Characterization of dilution systems for particle loss and transmission has been outlined elsewhere in our earlier work.[30] After dilution, the PM samples were independently measured by two aerosol instruments, an electrical low-pressure impactor (ELPI; Dekati Ltd.) and a scanning mobility particle sizer (SMPS; TSI, Inc.). The ELPI is a real-time size spectrometer that measures PSD in the range of 0.03–10 μm with 12 channels. The SMPS consists of a differential mobility analyzer (DMA; Model 3081), an electrostatic classifier (Model 3080), and a condensation particle counter (CPC; Model 3022A). It measures particles in the size ranges of 10–422 nm.

To investigate the effect of soft X-ray irradiation on ultrafine particle capture, a cylindrical-wire ESP developed by Washington University (denoted as WU-ESP) was used with a mounted soft X-ray emitter (Model L6941, Hamamatsu Photonics Ltd.) as shown in Figure 1. The WU-ESP had a stainless steel outer collecting electrode 15 cm in length and 5 cm in diameter. Varying voltages were applied to the central wire electrode of the WU-ESP using a Bertan high voltage power supply (Model 206-20, Spellman High Voltage Co.). The ion current generated after corona inception was measured using a microammeter connected to the WU-ESP ground electrode. A 2-cm circular hole was drilled through the middle of the collecting electrode to allow for soft X-ray irradiation penetration inside of the WU-ESP. X-ray irradiation (3.5–9.5 keV, λ = 0.12–0.41 nm) was spread inside of the ESP at an angle of approximately 120°. To prevent particles from depositing on the X-ray emitter and to keep the system airtight, a thin polyamide film (KaptonTM 30HN, DuPont Corp., 30-μm thick) was placed in front of the X-ray emitter.

The test plan is summarized in Table 1, which includes four sets of experiments. In sets I and II, ELPI and SMPS were used, respectively, to measure baseline PSDs at both EERC-ESP inlet and outlet. The particle collection efficiency of the EERC-ESP can be calculated from the inlet and outlet data. Set III was designed to test the performance of EERC-ESP in the scenario of sorbent injection as a strategy of capturing toxic metals. TTIP, the precursor of TiO_2 particles, was injected at 800 g/hr upstream of the EERC-ESP, where the flue gas temperature was approximately 900 °C. In set IV, a slipstream of flue gas was drawn at 5 L/min through WU-ESP at two levels of

Table 1. Summary of experimental conditions.

Set	PM Sampling Port	Aerosol Instrument	Operating Conditions	
I	EERC-ESP inlet and outlet	ELPI	Baseline	
II	EERC-ESP inlet and outlet	SMPS	Baseline	
III	EERC-ESP outlet	SMPS	Sorbent (TTIP) injection	
IV	EERC-ESP inlet and outlet[a]	SMPS	WU-ESP at −8.5 kV	Soft X-ray off
				Soft X-ray on
			WU-ESP at −10 kV	Soft X-ray off
				Soft X-ray on

Notes: PSDs are measured after WU-ESP.

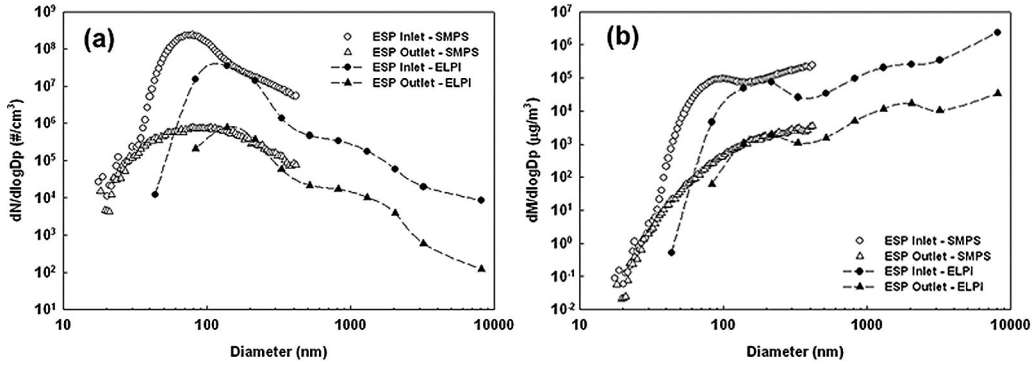

Figure 2. PSDs based on (a) number and (b) mass measured at the EERC-ESP inlet and outlet.

negative voltages (−8.5 and −10 kV). The soft X-ray was turned on and off and the enhancement of soft X-ray irradiation on particle capture was examined.

RESULTS AND DISCUSSION

Baseline PSDs and Particle Collection Efficiency

In the baseline tests (sets I and II), particle number and mass distribution data were collected at both EERC-ESP inlet and outlet and are shown in Figure 2. When converting to mass, a particle density of 1200 kg/m^3 was used. Information on particle shape was not available, and thus particles were assumed to be spherical. Note that errors may be associated with this assumption because fine particles from coal combustion are typically agglomerates with complex structures. The ELPI and SMPS data agreed with each other in part of the overlapping measurement range (150–300 nm). For particles in the nanosize (<100 nm) range, SMPS gave one order of magnitude higher concentration than ELPI at the EERC-ESP inlet, but the difference between SMPS and ELPI was much less significant at the EERC-ESP outlet. This difference can be contributed by the systematic error of the two aerosol instruments because they are based on different operating principles. In addition, because different sampling flow rates were used for the two instruments (SMPS = 0.3 L/min; ELPI = 10 L/min) and the dilution gas flow rate remained constant (40 L/min), the dilution ratio of the PM samples for SMPS was much higher than that for ELPI. Meanwhile, the residence time in the dilution chamber was the same (1.2–1.5 sec) for both measurements. At the relatively low sampling temperature (150 °C) all of the ash-forming compounds have already been condensed, and thus, it was not likely that nucleation or condensation would happen inside of the dilution chamber. However, coagulation can be strongly affected by dilution rate at a certain residence time. A lower dilution ratio for ELPI leads to a higher initial particle concentration in the dilution chamber. As a result, particles may shift to larger sizes and lower number concentrations because of coagulation when measured by ELPI compared with SMPS. This observation is consistent with the results reported in the literature. Lipsky et al.[31] reported that residence time and dilution rates do not influence particle mass emission rates from coal combustion but affect the size distributions and number concentrations because of coagulation (e.g., ultrafine particle concentration is higher at a larger dilution ratio). In another study by Lipsky et al.,[32] they indicated that, when sampling after the baghouse, the PSD and total particle number emission rate do not depend on the dilution ratio because of the much lower particle number concentrations in diluted samples and the absence of nucleation. This agrees with the results in this study that the PSDs measured by SMPS and ELPI did not vary much at the outlet of EERC-ESP despite the very different dilution ratios.

At the EERC-ESP inlet, many ultrafine particles were observed and the mode particle size based on number concentration was around 75 nm (Figure 2a). The mass concentrations at the EERC-ESP inlet followed a trimodal distribution (Figure 2b), although the modes did not stand out prominently when plotted in logarithmic scale. The three modes are at around 80–100 nm, 1–2 μm, and 10 μm, representing ultrafine particle mode, accumulation mode, and coarse particle mode, respectively. The PSD result was in agreement with typical coal combustion PSDs reported in the literature.[7–10] At the EERC-ESP outlet, the PSDs followed a similar trend as those measured at the EERC-ESP inlet but with a lower number and mass concentration for particles larger than 40 nm. For particles smaller than 40 nm, the difference between inlet and outlet concentration was not significant, indicating significant penetration. Quantitatively, the particle penetration through the ESP at a certain particle size (d_p) can be calculated as:

$$P(d_p) = \frac{N_{out}}{N_{in}} \quad (1)$$

where N_{in} and N_{out} are particle number concentrations (# cm^{-3}) of particles of size d_p at the ESP inlet and outlet, respectively. The data for particles less than 32 nm exhibited significant scatter (Figure 2), possibly because of very low particle concentration, and thus they were not included in the penetration calculation. Figure 3 shows the penetration as a function of particle size. The lowest penetration (P = 0.002) occurred around 70 nm. For particles larger than 70 nm, the penetration increased as particle size increased, and reached a plateau (P = ~0.015) in the range of 150–400 nm measured by the SMPS. The maximum penetration observed in this size range is consistent with that reported in the literature;[16–18] however, for the ELPI data the highest penetration occurred at approximately 2 μm. Again, the discrepancy between the SMPS

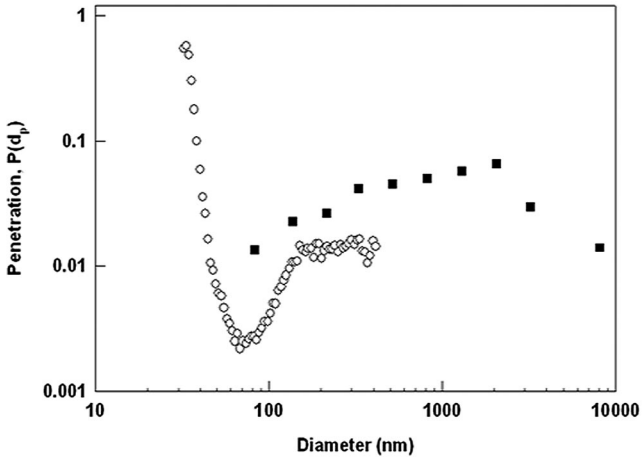

Figure 3. Particle penetration of EERC-ESP as a function of particle size (○, data from SMPS; ■, data from ELPI).

and ELPI results is likely because of the smaller dilution rate used by ELPI, in which the curve of N_{in} (at ESP inlet) for ELPI has shifted toward the right (larger particle size) because of coagulation. For particles smaller than 70 nm, the penetration increased as the size decreased. The penetration increased to approximately 0.01 at 50 nm and reached high values ($P = 0.55$) at 32 nm. The results are consistent with those from laboratory-scale studies in which significant particle penetration was observed when particles were smaller than 50 nm.[13,18,19]

Effect of Sorbent Injection on PSDs

In set III experiments, TTIP was sprayed through a precalibrated nozzle into the flue gas upstream of the EERC-ESP, where the gas temperature was approximately 900 °C. The TTIP droplets decomposed at this high temperature, forming TiO_2 particles. TTIP was injected at 800 g/hr, which resulted in a total TiO_2 particle concentration of 1.07 g/N · m³. During the 2-hr period of sorbent injection, the operation of EERC-ESP was apparently not affected because the sorbent-to-ash mass ratio was not significant (<0.1). Figure 4 compares the PSDs at both the EERC-ESP inlet and outlet under baseline (without sorbent injection) and sorbent injection conditions, respectively. With sorbent injection, the particle number concentration at the EERC-ESP inlet was an order of magnitude higher than that in the baseline for almost the entire size range. At the EERC-ESP outlet, the TTIP injection caused significant penetration of particles that were smaller than 100 nm. With TTIP injection, the mode concentration (at 55 nm) was 4 times higher than the baseline, and the total number concentration was 2.5 times higher than the baseline. The charging characteristics of the sorbent particles may also be different (TiO_2 is a highly resistive material), resulting in lower capture. The results indicate that proper design considerations must be taken into account to ensure that nanostructured sorbents used for pollutant removal do not escape collection in the ESP system. Appropriate injection rates of sorbents can ensure that the sizes are appropriate for effective capture in ESPs.

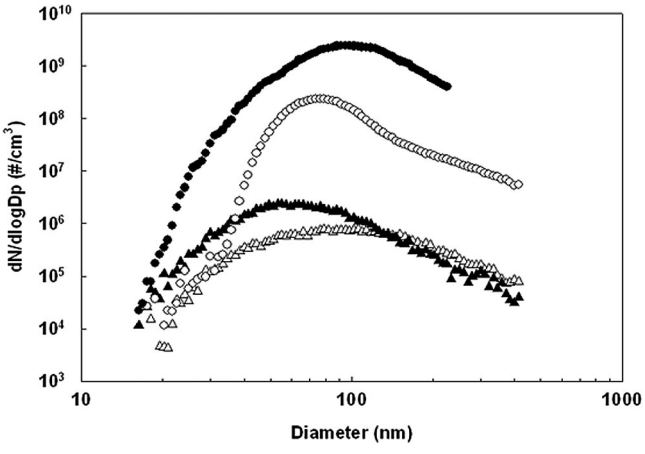

Figure 4. Comparison of PSDs with and without sorbent injection (○, EERC-ESP inlet baseline; ●, EERC-ESP inlet with TTIP injection; △, EERC-ESP outlet baseline; ▲, EERC-ESP outlet with TTIP injection).

Effect of Soft X-Ray Irradiation on Particle Capture

In set IV experiments, a slipstream of flue gas was introduced to the WU-ESP with the soft X-ray emitter. The SMPS was used to measure the PSD after the WU-ESP, and the effect of the soft X-ray irradiation was examined. Generally, at a given voltage of the WU-ESP, the measured current with the presence of soft X-ray irradiation is significantly higher than without. Estimated ion concentrations with and without soft X-ray were on the order of 10^{14} and 10^{12} cm^{-3}, respectively, when the WU-ESP was operated at −8.5 kV. Operational details of the WU-ESP coupled with soft X-ray, as well as the current-voltage characteristics, have been reported in our previous studies.[20,26]

Figure 5 shows the effects of ESP voltage and soft X-ray radiation on particle penetration calculated by eq 1. The slipstream was first introduced from the EERC-ESP inlet and the results are shown in Figure 5a. When the soft X-ray was off and the WU-ESP was operated at −8.5 kV, its inception voltage (the voltage at which the current starts increasing at a much faster rate because of formation of the corona), the performance of the WU-ESP was similar to the EERC-ESP. The particle penetration reached a minimum ($P \approx 0.001$) in the range of 50–80 nm, increased slightly when the particle size was greater than 80 nm, and increased dramatically when the particle size decreased below 50 nm ($P = 0.07$ at 30 nm). This result again verified that ultrafine particles, especially particles less than 50 nm, are difficult to capture by ESPs. When the soft X-ray was turned on with the WU-ESP operated at −8.5 kV, the particle penetration decreased significantly throughout the measured size range, attributable to the enhanced charging of particles under X-ray radiation. The mechanism of charging the particles is due to the enhanced ion concentration and direct photoionization. However, with increasing the applied voltage to −10 kV, a very low penetration was observed for all sizes, similar to the −8.5 kV with soft X-ray irradiation. Hence, an increased ion concentration region in a small-scale ESP can also enhance the capture of the particles smaller than 50 nm. However, this is not feasible in larger scale ESPs, as

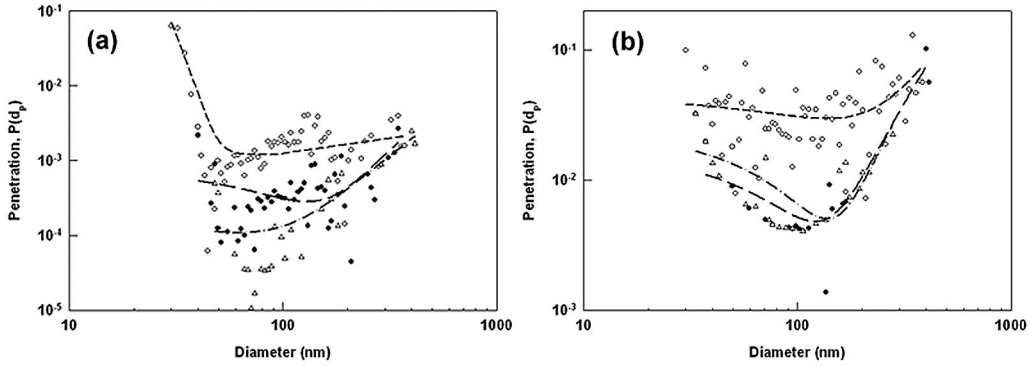

Figure 5. Effects of ESP voltage and soft X-ray irradiation on particle penetration through the WU-ESP with slipstream drawn from (a) the EERC-ESP inlet and (b) the EERC-ESP outlet (short dashed line and ○, −8.5 kV with X-ray off; long dashed line and ●, −8.5 kV with X-ray on; dash-dot line and △, −10 kV with X-ray off).

has been demonstrated in our earlier measurements and the few other pilot-scale studies. Increase of applied voltage also increases power requirements and enhances instability of operation because of sparking. Thus, the use of photoionization systems such as the soft X-ray would be very beneficial at enhancing ultrafine particle capture with low power consumption and increased stability of the corona. Experiments with soft X-ray and the higher voltage (−10 kV) resulted in an interesting observation—the creation of a large number of particles. This could be due to the soft X-ray neutralizing the ions, resulting in a decrease in charging efficiency; or a large number of ions escaping the ESP and entering the particle measurement device (CPC), resulting in new particle formation due to ion-induced nucleation. Controlled studies in the laboratory could not duplicate this observation of enhanced particle formation with soft X-ray irradiation at high voltages (−10 kV). More studies are necessary to firmly understand the performance of the soft X-ray under high voltage conditions in which ion concentrations are very high. Clearly the use of a soft X-ray system would not require the use of higher voltages; hence, this may not be a very important aspect.

Figure 5b shows the results when the slipstream was introduced to the WU-ESP from the EERC-ESP outlet, where the particle concentration was much lower than that from the EERC-ESP inlet. Applying a voltage of −8.5 kV to the WU-ESP resulted in an average particle penetration of $P \approx 0.04$ for particles smaller than 200 nm. Either turning on the X-ray or increasing the voltage to −10 kV caused a remarkable decrease in particle penetration ($P < 0.01$) for particles smaller than 200 nm. The unusual large number of particles were detected again when turning the soft X-ray on at −10 kV ESP voltage.

CONCLUSIONS

The PSDs in the range of 17 nm to 10 μm were measured in a pilot-scale (EERC) pulverized coal combustor burning a PRB subbituminous coal. At the EERC-ESP inlet, high number concentrations of ultrafine particles were observed with the mode around 75 nm. The mass concentrations at the EERC-ESP inlet followed a trimodal distribution with the modes at around 80–100 nm, 1–2 μm, and 10 μm. The penetration of ultrafine particles increased as particle size decreased below 70 nm; and significant penetration was observed for particles smaller than 50 nm. Injection of fine-particle sorbents as a strategy of capture toxic metals in the flue gas needs to be designed carefully to ensure that the sorbent particles are captured in the ESP. Insufficient or partial charging of the ultrafine particles caused a decrease in their collection efficiency. The WU-ESP, which is mounted with a soft X-ray emitter, was used for slipstream studies and the effect of X-ray irradiation on particle capture was examined. At relatively low electrode voltages (−8.5 kV), the soft X-ray significantly enhanced particle charging and collection efficiency.

ACKNOWLEDGMENTS

This work was supported by the U.S. Department of Energy grant no. DE-FGZ6-05NT42531 and Ameren UE, St. Louis, through contract no. W-0001-06, Missouri Department of Natural Resources.

REFERENCES

1. Biswas, P.; Wu, C.Y. Critical Review: Nanoparticles and the Environment; *J. Air & Waste Manage. Assoc.* **2005**, *55,* 708-746.
2. Liao, D.P.; Creason, J.; Shy, C.; Williams, R.; Watts, R.; Zweidinger, R. Daily Variation of Particulate Air Pollution and Poor Cardiac Autonomic Control in the Elderly; *Environ. Health Perspect.* **1999**, *107,* 521-525.
3. Samet, J.M.; Dominici, F.; Curriero, F.C.; Coursac, I.; Zeger, S.L. Fine Particulate Air Pollution and Mortality in 20 U.S. Cities, 1987–1994; *N. Engl. J. Med.* **2000**, *343,* 1742-1749.
4. Seaton, A.; Macnee, W.; Donaldson, K.; Godden, D. Particulate Air-Pollution and Acute Health-Effects; *Lancet* **1995**, *345,* 176-178.
5. National Ambient Air Quality Standards for Particulate Matter. *Fed. Regist.* **1997**, *62,* 38652.
6. Davidson, C.I.; Phalen, R.F.; Solomon, P.A. Airborne Particulate Matter and Human Health: a Review; *Aerosol Sci. Technol.* **2005**, *39,* 737-749.
7. Zhuang, Y.; Biswas, P. Submicrometer Particle Formation and Control in a Bench-Scale Pulverized Coal Combustor; *Energy Fuels* **2001**, *15,* 510-516.
8. Chang, M.C.O.; Chow, J.C.; Watson, J.G.; Hopke, P.K.; Yi, S.M.; England, G.C. Measurement of Ultrafine Particle Size Distributions from Coal-, Oil-, and Gas-Fired Stationary Combustion Sources; *J. Air & Waste Manage. Assoc.* **2004**, *54,* 1494-1505.
9. Linak, W.P.; Miller, C.A. Comparison of Particle Size Distributions and Elemental Partitioning from the Combustion of Pulverized Coal and Residual Fuel Oil; *J. Air & Waste Manage. Assoc.* **2000**, *50,* 1532-1544.
10. Yoo, J.I.; Seo, Y.C.; Shinagawa, T. Particle-Size Distributions and Heavy Metal Partitioning in Emission Gas from Different Coal-Fired Power Plants; *Environ. Eng. Sci.* **2005**, *22,* 272-279.
11. Quann, R.J.; Neville, M.; Sarofim, A.F. A Laboratory Study of the Effect of Coal Selection on the Amount and Composition of Combustion Generated Submicron Particles; *Combust. Sci. Tech.* **1990**, *74,* 245-265.

12. Senior, C.L.; Bool, L.E.; Srinivasachar, S.; Pease, B.R.; Porle, K. Pilot Scale-Study of Trace Element Vaporization and Condensation during Combustion of a Pulverized Sub-Bituminous Coal; *Fuel Process. Technol.* **2000**, *63,* 149-165.
13. Huang, S.H.; Chen, C.C. Ultrafine Aerosol Penetration through Electrostatic Precipitators; *Environ. Sci. Technol.* **2002**, *36,* 4625-4632.
14. Hinds, W.C. *Aerosol Technology: Properties, Behavior, and Measurement of Airborne Particles*; Wiley-Interscience: New York, 1982.
15. Friedlander, S.K. *Smoke, Dust, and Haze: Fundamentals of Aerosol Dynamics*; Oxford: Oxford, U.K., 2000.
16. Senior, C.L.; Helble, J.J.; Sarofim, A.F. Emissions of Mercury, Trace Elements, and Fine Particles from Stationary Combustion Sources; *Fuel Process. Technol.* **2000**, *65,* 263-288.
17. Ylatalo, S.I.; Hautanen, J. Electrostatic Precipitator Penetration Function for Pulverized Coal Combustion; *Aerosol Sci. Technol.* **1998**, *29,* 17-30.
18. Yoo, K.H.; Lee, J.S.; Oh, M.D. Charging and Collection of Submicron Particles in Two-Stage Parallel-Plate Electrostatic Precipitators; *Aerosol Sci. Technol.* **1997**, *27,* 308-323.
19. Zhuang, Y.; Kim, Y.J.; Lee, T.G.; Biswas, P. Experimental and Theoretical Studies of Ultra-Fine Particle Behavior in Electrostatic Precipitators; *J. Electrostat.* **2000**, *48,* 245-260.
20. Suriyawong, A.; Hogan, C.J.; Jiang, J.K.; Biswas, P. Charged Fraction and Electrostatic Collection of Ultrafine and Submicrometer Particles Formed during O_2-CO_2 Coal Combustion; *Fuel* **2008**, *87,* 673-682.
21. McCain, J.D.; Gooch, J.P.; Smith, W.B. Results of Field Measurements of Industrial Particulate Sources and Electrostatic Precipitator Performance; *J. Air Poll. Control Assoc.* **1975**, *25,* 117-121.
22. Biswas, P.; Wu, C.Y. Control of Toxic Metal Emissions from Combustors Using Sorbents: a Review; *J. Air & Waste Manage. Assoc.* **1998**, *48,* 113-127.
23. Lee, T.G.; Biswas, P.; Hedrick, E. Comparison of Hg^0 Capture Efficiencies of Three in Situ Generated Sorbents; *AICHE J.* **2001**, *47,* 954-961.
24. Wu, C.Y.; Lee, T.G.; Tyree, G.; Arar, E.; Biswas, P. Capture of Mercury in Combustion Systems by in Situ-Generated Titania Particles with UV Irradiation; *Environ. Eng. Sci.* **1998**, *15,* 137-148.
25. Lee, T.G.; Hyun, J.E. Structural Effect of the in Situ Generated Titania on its Ability to Oxidize and Capture the Gas-Phase Elemental Mercury; *Chemosphere* **2006**, *62,* 26-33.
26. Kulkarni, P.; Namiki, N.; Otani, Y.; Biswas, P. Charging of Particles in Unipolar Coronas Irradiated by in-Situ Soft X-Rays: Enhancement of Capture Efficiency of Ultrafine Particles; *J. Aerosol Sci.* **2002**, *33,* 1279-1296.
27. Hogan, C.J.; Lee, M.H.; Biswas, P. Capture of Viral Particles in Soft X-Ray-Enhanced Corona Systems: Charge Distribution and Transport Characteristics; *Aerosol Sci. Technol.* **2004**, *38,* 475-486.
28. Jiang, J.; Lee, M.H.; Biswas, P. Model for Nanoparticle Charging by Diffusion, Direct Photoionization, and Thermionization Mechanisms; *J. Electrostat.* **2007**, *65,* 209-220.
29. Lee, H.M.; Kim, C.S.; Shimada, M.; Okuyama, K. Bipolar Diffusion Charging for Aerosol Nanoparticle Measurement Using a Soft X-Ray Charger; *J. Aerosol Sci.* **2005**, *36,* 813-829.
30. Biswas, P. Measurement of High Concentration and High Temperature Aerosols. In *Aerosol Measurement: Principles, Techniques and Applications*, Baron, P., Willeke, K., Eds.; John Wiley and Sons: New York, 2001; pp 903-928.
31. Lipsky, E.; Stanier, C.O.; Pandis, S.N.; Robinson, A.L. Effects of Sampling Conditions on the Size Distribution of Fine Particulate Matter Emitted from a Pilot-Scale Pulverized-Coal Combustor; *Energy Fuels* **2002**, *16,* 302-310.
32. Lipsky, E.M.; Pekney, N.J.; Walbert, G.F. O'Dowd, W.J.; Freeman, M.C.; Robinson, A. Effects of Dilution Sampling on Fine Particle Emissions from Pulverized Coal Combustion; *Aerosol Sci. Technol.* **2004**, *38,* 574-587.

About the Authors

Ying Li is a postdoctoral fellow, Achariya Suriyawong and Michael Daukoru are doctoral students, and Pratim Biswas is the Stifel and Quinette Jens Professor and Chair in the Department of Energy, Environmental, and Chemical Engineering at Washington University in St. Louis. Ye Zhuang is a senior engineer in the EERC at the University of North Dakota. Please address correspondence to: Pratim Biswas, Aerosol and Air Quality Research Lab, Campus Box 1180, St. Louis, MO 63130; phone: +1-314-935-5548; fax: +1-314-935-5464; e-mail: pratim.biswas@wustl.edu.